Urologia Internationalis

Research Article

Urol Int 2023;107:632–645
DOI: 10.1159/000527873

Received: November 16, 2021
Accepted: September 21, 2022
Published online: March 23, 2023

Hsa_circ_0008035 Knockdown Inhibits Bladder Cancer Progression through miR-1184/RAP2B Axis

Yang Fu Kun Liu Xi Jiang Lun Zhao Tianwei Wang

Department of Urology, The Affiliated Huaian No. 1 People's Hospital of Nanjing Medical University, Huai'an, China

Keywords
Bladder cancer · hsa_circ_0008035 · miR-1184 · RAP2B · Angiogenesis

Abstract
Introduction: Circular RNAs (circRNAs) are related to the pathogenesis and progression of bladder cancer (BC). This research aimed to investigate the role and mechanism of hsa_circ_0008035 (circ_0008035) in BC progression. ***Methods:*** Circ_0008035, microRNA (miR)-1,184, and Ras-related protein 2B (RAP2B) levels were examined in BC via quantitative real-time polymerase chain reaction and Western blotting. Cell Counting Kit-8, colony formation, 5-ethynyl-2′-deoxyuridine staining, flow cytometry, caspase-3 assay kit, transwell, and tube formation assays were conducted to estimate the effects of circ_0008035 on the malignant phenotypes of BC tumors. The interaction between RNAs and genes was evaluated via a dual-luciferase reporter and RNA immunoprecipitation assays. A xenograft model of BC in nude mice was established to estimate the effect of circ_0008035 in BC in vivo. ***Results:*** Circ_0008035 and RAP2B levels were upregulated, while miR-1184 abundance was downregulated in BC tissues and cells. Circ_0008035 knockdown constrained cell proliferation, migration, invasion and angiogenesis but promoted apoptosis in vitro. And circ_0008035 silencing curbed xenograft tumor growth in vivo. Circ_0008035 acted as a miRNA sponge for miR-1184. Circ_0008035 increased RAP2B expression by sponging miR-1184. MiR-1184 downregulation relieved the effects of circ_0008035 knockdown on BC progression. And RAP2B knockdown partly reversed the effects of miR-1184 overexpression on BC progression. ***Conclusion:*** Circ_0008035-mediated BC progression via regulating the miR-1184/RAP2B axis, providing a potential target for BC treatment.

Introduction

Bladder cancer (BC) is the most common urinary cancer in men, 75% of which is identified as non-muscle-invasive [1]. Transitional cell carcinoma (TCC), also known as urothelial carcinoma, is the most common type of BC [2]. There are about 430,000 new BC cases and 165,000 cancer-related deaths worldwide [3]. Despite the great advances made in therapeutic methods of BC, the overall clinical outcome remains poor [4]. Thus, exploring the molecular mechanisms of carcinogenesis and the progression of BC may be helpful for BC treatment.

Noncoding RNAs are related to the occurrence and development of BC, and noncoding RNA represents a potential diagnostic and therapeutic strategy for cancer treatment [5]. Circular RNAs (circRNAs), with unique closed structures, are related to the tumorigenesis of BC

Karger@karger.com
www.karger.com/uin

Correspondence to:
Kun Liu, hyliukun@126.com

Table 1. Correlation between clinicopathological features and hsa_circ_0008035 expression levels in BC patients (transitional cell carcinom)

Clinical feature	*n*	hsa_circ_0008035		*p* value
		high	low	
Age				
≥60	30	14	16	0.6936
<60	25	13	12	
Gender				
Man	33	17	16	0.6596
Woman	22	10	12	
Tumor size				
≥3 cm	24	14	10	0.2277
<3 cm	31	13	18	
TNM stage				
III + IV	34	20	14	0.0662
I + II	21	7	14	
Lymph node metastasis				
N0	40	15	25	0.0050
N1	15	12	3	
Distant metastasis				
M0	43	18	25	0.0423
M1	12	9	3	

Table 2. The oligo sequences for cell transfection

Name	Sequence (5′-3′)
si-circ_0008035#1	AGCAAGGUAUGAUUAUCGGGA
si-circ_0008035#2	AGAGCAAGGUAUGAUUAUCGG
si-NC	UCAUACGAACGAGAGAGGAA
miR-1184 mimic	CCUGCAGCGACUUGAUGGCUUCC
NC	CGAUCGCAUCAGCAUCGAUUGC
anti-miR-1184	GGAAGCCAUCAAGUCGCUGCAGG
anti-NC	CUAACGCAUGCACAGUCGUACG

[6]. Moreover, circRNAs function as competitive endogenous RNAs (ceRNAs) by interacting with microRNAs (miRNAs) to regulate the target gene expression, thus taking part in tumor development [7]. For example, hsa_circ_0001944 contributes to cell growth and metastasis in BC via serving as a ceRNA for miR-548 to modulate prokineticin-2 [8]. Furthermore, hsa_circ_0071196/miR-19b-3p/citron Rho-interacting serine/threonine kinase ceRNA network promotes proliferation and migration of BC [9]. Hsa_circ_0008035 (circ_0008035) is a circRNA derived from exostosin glycosyltransferase 1 (EXT1) that is formed by back-splicing of exon 5–10, which is upregulated in BC patients [10]. Nevertheless, the potential function and mechanism of circ_0008035 in BC progression remain unknown.

MiRNAs, a class of noncoding RNAs, exerted key roles in diagnosis, prognosis, and treatment of patients with BC [11]. MiRNAs are relevant to various cellular processes in BC [12]. A previous research indicated that miR-1184 inhibition can promote cell proliferation, migration, and invasion in BC [13]. But whether miR-1184 participates in the regulation of circ_0008035 in BC development is unknown. Ras-related protein 2B (RAP2B) is a member of the Ras family, which is activated by p53 and inhibits p53-mediated apoptosis [14]. Moreover, a previous study shows that miR-194 can play as a tumor suppressor to repress cell proliferation and invasion via downregulating RAP2B in BC [15].

This study focused on the function of circ_0008035 on cell proliferation, apoptosis, migration, invasion, and angiogenesis. Moreover, we investigated the regulatory network of circ_0008035/miR-1184/RAP2B in BC, hoping to provide a novel therapeutic target for BC.

Materials and Methods

Patients and Tissues

In this research, 55 BC patients were recruited in the Affiliated Huaian No. 1 People's Hospital of Nanjing Medical University. The tumor specimens and adjacent normal tissues (>3 cm from tumor) were harvested from BC patients and stored in liquid nitrogen for RNA extraction. All samples were transitional cell carcinoma. None of the patients received any treatment before surgery. The clinicopathological features of BC patients are shown in Table 1. The written informed consents were obtained from all of the patients. This research was conducted in accordance with the Declaration of Helsinki and was approved by the Affiliated Huaian No. 1 People's Hospital of Nanjing Medical University. The gene expression profile GSE92675 of BC samples was downloaded from the Gene Expression Omnibus (GEO) database (http://www.ncbi.nlm.nih.gov/geo) and was analyzed using Agilent-069978 Arraystar Human CircRNA Microarray V1 (Agilent Technologies, Santa Clara, CA, USA).

Cell Culture and Transfection

Human ureteral epithelial cells (SV-HUC-1), human BC cell lines (5,637 and T24), and human umbilical vein endothelial cells (HUVECs) were purchased from Procell (Wuhan, China), and grown in RPMI-1640 medium (Gibco, Grand Island, NY, USA) plus 10% fetal bovine serum (Gibco) and 1% penicillin/streptomycin (Gibco) at 37°C under 5% CO_2.

Circ_0008035 sequences were inserted into the pCD5-ciR vector to construct the circ_0008035 overexpression vector, and the empty pCD5-ciR vector was used as a negative control (circ-NC) (Guangzhou, China). RAP2B overexpression vector was generated using the pcDNA3.1 vector, and the empty pcDNA3.1

Table 3. The primer sequences for qRT-PCR

Name	Sequence (5′-3′)	
	forward	reverse
miR-1184	GCCGAGCCTGCAGCGACTTGA	AGTGCAGGGTCCGAGGTATT
U6	GCTCGCTTCGGCAGCACA	AACGCTTCACGAATTTGCGT
circ_0008035	GGAATTGTGACAAGCCCCTA	CAAAGCCTCCAGGAATCTGA
EXT1	CGTGCCTCTTTGTCCTGAGT	ATGTCAAACCCCACGTCCTC
RAP2B	AGCCTCGGTAGACGAGCTAT	TCGGATGCGTTTGGCTTTTG
18S rRNA	ACCCGTTGAACCCCATTCGTGA	GCCTCACTAAACCATCCAATC

vector was used as the negative control (vector). Small interfering RNA (siRNA) against circ_0008035 (si-circ_0008035#1 and si-circ_0008035#2), siRNA negative control (si-NC), miR-1184 mimic, miRNA negative control (NC), miR-1184 inhibitor (anti-miR-1184), and inhibitor negative control (anti-NC) were obtained from Genepharma (Shanghai, China). The oligo sequences are shown in Table 2. In brief, 30 nM oligos or 600 ng vectors were transfected into 5,637 and T24 cells with Lipofectamine™ 2,000 (Thermo Fisher Scientific, Waltham, MA, USA). 24 h upon transfection, the cells were collected for further investigation.

Quantitative Real-Time Polymerase Chain Reaction

Total RNA was extracted with Trizol (Vazyme, Nanjing, China) following the manufacturer's instructions and quantified using a NanoDrop ND-2000 spectrophotometer (Thermo Fisher Scientific). The nuclear or cytoplasmic RNA was obtained using the Cytoplasmic & Nuclear RNA Purification kit (Norgen Biotek, Thorold, Canada). The samples (1 μg) with an optical density (OD) 260/280 between 1.8 and 2.0 were selected for reverse transcription using the All-in-One™ cDNA synthesis kit (FulenGen, Guangzhou, China). The quantitative real-time polymerase chain reaction (qRT-PCR) was conducted with cDNA templates, special primers, and SYBR Green (TaKaRa, Dalian, China). The primers are generated by Sangon Biotech (Shanghai, China) and listed in Table 3. The relative level of RNA was normalized to 18S rRNA or U6, and calculated according to the $2^{-\Delta\Delta Ct}$ method [16].

RNase R Treatment

Extracted RNA was treated with 2 U/μg RNase R (Geneseed) at 37°C for 20 min. Circ_0008035 and EXT1 levels were examined via qRT-PCR.

Cell Counting Kit-8

5,637 and T24 cells (3×10^3 cells per well) were added in 96-well plates in triplicate. After the culture of 0, 24, 48, and 72 h, cells were incubated with Cell Counting Kit-8 reagent (Beyotime, Shanghai, China) for 3 h. The OD value of each well at 450 nm was determined through microplate reader (Bio-Rad, Hercules, CA, USA).

Colony Formation Analysis

5,637 and T24 cells (500 cells/well) were added in 6-well plates. After culture for 10 days, cells were stained using 0.5% crystal violet (Beyotime) for 10 min and imaged. The colony formation ability was calculated by normalizing to the control group.

5-Ethynyl-2′-Deoxyuridine Staining

Cell proliferation was tested through the BeyoClick™ 5-Ethynyl-2′-Deoxyuridine (Edu) Cell Proliferation Kit with Alexa Fluor 488 (Beyotime). In brief, 4×10^4 5,637 and T24 cells were added in 24-well plates. After incubation for 24 h, cells were interacted with 10 μM Edu for 2 h and subjected to fixing with 4% paraformaldehyde (Beyotime) and treatment with 0.3% Triton X-100 (Beyotime). Then the cells were incubated with the click reaction solution for 30 min. Hoechst 33342 was used to label the nuclei. Cells were observed through a fluorescence microscope (Olympus, Tokyo, Japan).

Flow Cytometry

1×10^5 5,637 and T24 cells were added in 12-well plates and incubated for 72 h. After fixing using 75% ethanol (Aladdin, Shanghai, China), cells were interacted with propidium iodide (PI; Beyotime). Cycle process was examined with a flow cytometer (Becton Dickinson, San Jose, CA, USA).

Annexin V-FITC/PI apoptosis detection kit (Sigma-Aldrich) was used for cell apoptosis assay through flow cytometry. Transfected 5,637 and T24 cells (5×10^4 cells) were seeded in 6-well plates and cultured for 72 h. Then the collected cells were dyed with Annexin V-FITC and PI in the dark for 10 min. The apoptotic cells (Annexin V-FITC and PI-positive) were examined with a flow cytometer.

Caspase-3 Activity Assay

Caspase-3 activity was examined using a caspase-3 activity assay kit (Beyotime). Briefly, 2×10^5 5,637 and T24 cells were added in 6-well plates. After 72 h, cells were lysed and incubated with 2 mM Ac-DEVD-pNA at 37°C for 2 h. The OD level at 405 nm was examined through a microplate reader. Relative caspase-3 activity was calculated via normalizing to the control group.

Transwell Assay

Cell migration and invasion were measured using 24-well transwell chambers (Becton Dickinson), which were precoated via Matrigel (Solarbio) for invasion assay. Briefly, transfected 5,637 and T24 cells (1×10^4 for migration assay, and 5×10^4 for invasion assay) were re-suspended in serum-free medium and seeded into upper chambers. The lower chamber was added with 500 μL medium containing 10% fetal bovine serum. After culture for 24 h at 37°C, cells on the topside were removed, and those penetrating the membrane were dyed with 0.5% crystal violet for 3 min. The stained cells were observed and photographed under a microscope (×200 magnification, Olympus).

Tube Formation Analysis

HUVECs (2×10^4) were added in 96-well plates coated with Matrigel overnight. The culture medium of assigned 5,637 and T24 cells was collected, centrifuged, and filtered to obtain tumor-conditioned medium (TCM). Pre-starved HUVECs were then co-cultured with TCM for 24 h. Finally, the formation of tubular structure was observed with an inverted microscope, and it was expressed as a fold in the control group.

Dual-Luciferase Reporter and RNA Immunoprecipitation (RIP) Assays

Bioinformatics software circinteractome (https://circinteractome.irp.nia.nih.gov/) and TargetScan (http://www.targetscan.org/vert_71/) were applied to predict the targets of circ_0008035 or miR-1184. Wild-type (wt) sequences of circ_0008035 or RAP2B 3′UTR harboring the putative binding sites of miR-1184 were amplified and cloned in pmirGLO vectors (Promega, Madison, WI, USA) to generate circ_0008035-wt or RAP2B-wt. And circ_0008035 or RAP2B 3′UTR sequences containing mutant (mut) miR-1184 binding sites were cloned in pmirGLO vectors and named circ_0008035-mut or RAP2B-mut. Cells with 60% confluence were co-transfected with the mentioned luciferase reporter vectors and miR-1184 mimic or NC. 24 h upon transfection, cells were harvested for dual-luciferase activity analysis using a dual-luciferase reporter assay kit (Promega).

RIP analysis was conducted using the Magna RIP kit (Sigma-Aldrich, St. Louis, MO, USA). The cell lysates of 1×10^7 5,637 and T24 cells were incubated with Ago2 or IgG-coated magnetic beads. After purification, the levels of circ_0008035, miR-1184, and RAP2B were examined via qRT-PCR.

Western Blotting

Cells or tissues were lysed with RIPA buffer (Yeasen, Shanghai, China) on ice and then centrifuged at 12, 000 g for 10 min for supernatant collection. The Enhanced BCA Protein Assay Kit (Beyotime) was used to detect the concentration of protein. Equal amounts of sample (20 μg) in sample loading buffer (Beyotime) were separated via SDS-PAGE and transferred on the nitrocellulose membranes (Bio-Rad). After blocking using QuickBlock™ Blocking Buffer (Beyotime), the membranes were interacted with primary antibodies, including anti-CDK1 (ab133327, 1:15,000, Abcam, Cambridge, UK), anti-Cyclin B1 (ab32053, 1:10,000, Abcam), anti-Cyclin D1 (ab16663, 1:200, Abcam), anti-Bcl-2 (ab182858, 1:2,000, Abcam), anti-Bax (ab32503, 1:5,000, Abcam), anti-cleaved caspase 3 (ab49822, 1:500), anti-cleaved caspase 8 (A11324, 1:1,000, Abclonal, Wuhan, China), anti-cleaved caspase 9 (ab2324, 1:800, Abcam), anti-MMP-7 (ab207299, 1:1,000, Abcam), anti-MMP-2 (ab92536, 1:5,000, Abcam), anti-MMP-9 (ab76003, 1:10,000, Abcam), anti-E-cadherin (ab40772, 1:20,000, Abcam), anti-N-cadherin (ab76011, 1:10,000, Abcam), anti-vimentin (ab8978, 1:2,000, Abcam), anti-RAP2B (ab101369, 1:1,000, Abcam), or anti-GAPDH (ab181602, 1:5,000, Abcam). Followed by incubating with Goat Anti-Rabbit IgG H&L (HRP) (ab6721, 1:8,000, Abcam). The visualization of protein signals was developed through BeyoECL Plus (Beyotime) and the densitometry analysis was carried out with Image Lab software (Bio-Rad).

Murine Xenograft Analysis

Lentiviral vectors-based sh-circ_0008035 or sh-NC were generated by FulenGen. The stably transfected 5,637 and T24 cells were selected via 5 μg/mL puromycin. The BALB/c nude mice (male, 5-week-old) were provided by Vital River (Beijing, China) and randomly divided into the sh-circ_0008035 or sh-NC group ($n = 5$). The mice were subcutaneously injected with 5,637 or T24 cells (5×10^6) stably transfected with sh-circ_0008035 or sh-NC. The procedures were permitted by the Animal Research Committee of the Affiliated Huaian No. 1 People's Hospital of Nanjing Medical University. Animal studies were performed in compliance with the ARRIVE guidelines and the Basel Declaration. All animals received humane care according to the National Institutes of Health (USA) guidelines. Tumor volume was detected weekly and calculated by $0.5 \times \text{width}^2 \times \text{length}$. Five weeks upon injection, all of the mice were euthanized by inhalation anesthesia of 5% isoflurane (Sigma-Aldrich), and tumors were weighted and harvested for further experiments.

Statistical Analysis

The experiments were repeated 3 times, and results were shown as mean ± standard deviation. Pearson's correlation analysis was used to investigate the correlation among circ_0008035, miR-1184, and RAP2B expression level in BC tissues. Statistical difference was analyzed using Student's *t* test or ANOVA via GraphPad Prism 7 software (GraphPad Inc., La Jolla, CA, USA). p value <0.05 is considered as significant difference.

Results

Circ_0008035 and RAP2B Levels Are Upregulated, and miR-1184 Expression Is Decreased in BC

To investigate the roles of circ_0008035, miR-1184, and RAP2B in BC, we first investigated their expression levels in BC. The expression value of circ_0008035 in samples from GSE92675 (four pairs of BC and matched non-cancer tissues) is displayed in Figure 1a, and circ_0008035 was highly expressed in tumors as compared to adjacent normal tissues. Subsequently, qRT-PCR analysis in 55 clinical samples was performed. Compared with adjacent normal tissues ($n = 55$), circ_0008035 expression was markedly increased in BC tissues ($n = 55$) (Fig. 1b). Besides, to assess the pathological relevance of circ_0008035 level in BC, we evaluated the correlation between circ_0008035 expression and the clinicopathological features of BC patients. As shown in Table 1, patients with high circ_0008035 expression were more susceptible to lymph node metastasis ($p = 0.0050$) and distant metastasis ($p = 0.0423$), while it had no correction with the age, gender, tumor size, and TNM stage of BC patients. Additionally, higher circ_0008035 expression was shown in BC cells (5,637, T24, UM-UC-3 and RT-4) in contrast with human ureteral epithelial cells (SV-HUC-1) (Fig. 1c; online Suppl. Fig. 2I; for all online suppl. material, see www.karger.com/doi/10.1159/000527873).

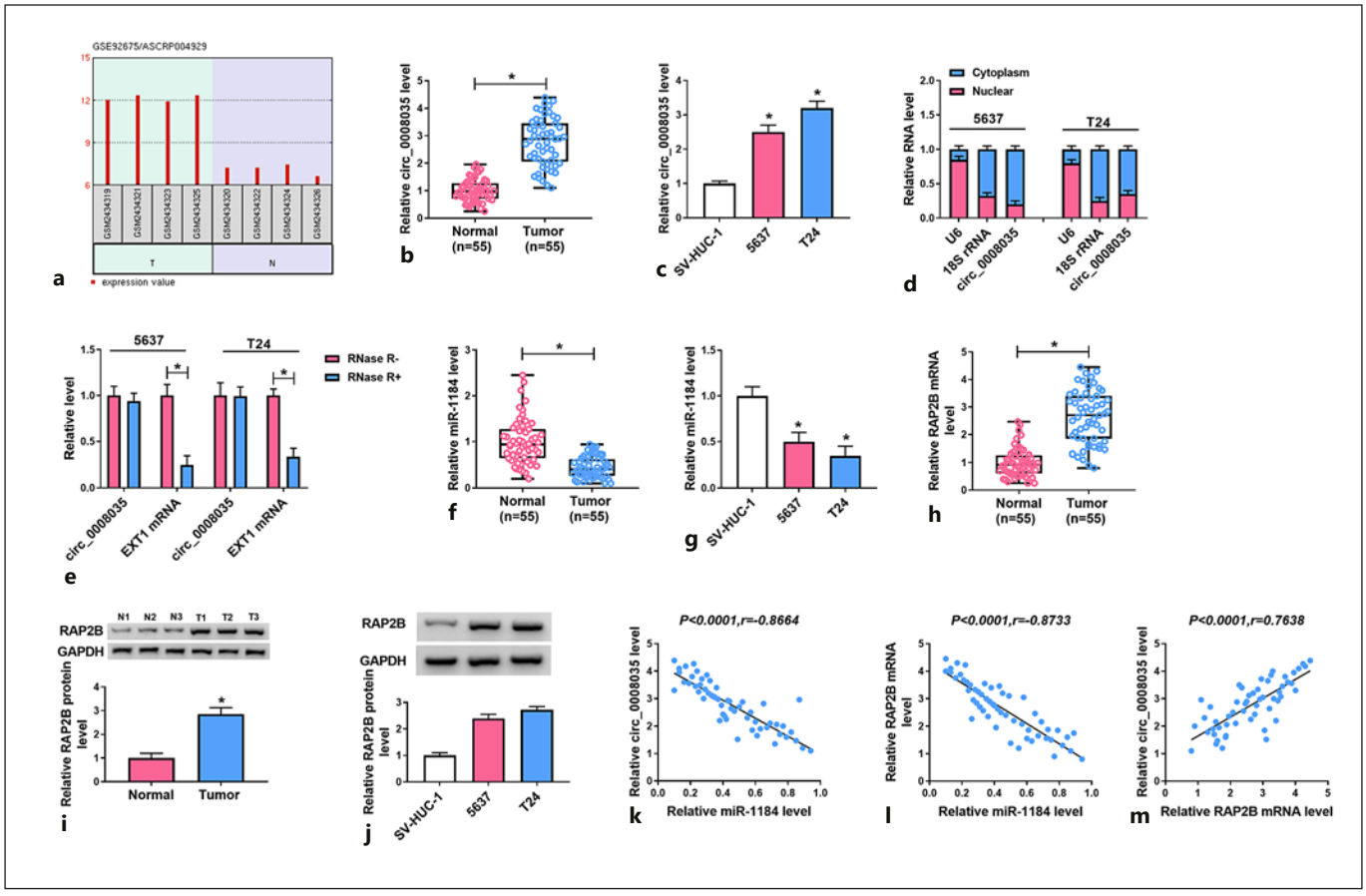

Fig. 1. Circ_0008035, miR-1184 and RAP2B expression in BC. **a** Circ_0008035 was highly expressed in tumor (T) as compared to adjacent normal tissues (N) in GSE92675. **b** Circ_0008035 abundance in 55 paired BC tumor tissues and adjacent normal tissues was examined by qRT-PCR. **c** Circ_0008035 level was detected using qRT-PCR in BC cells (5,637 and T24) and human ureteral epithelial cells (SV-HUC-1). **d** The nuclear and cytoplasm separation experiment was employed to explore the location of circ_0008035 in BC cells. **e** The levels of circ_0008035 and its linear transcript EXT1 mRNA in BC cells with or without RNase R treatment were measured by qRT-PCR. **f**, **g** MiR-1184 expression was detected by qRT-PCR in BC tissues ($n = 55$) and cells. **h**–**j** RAP2B mRNA and protein levels in BC tissues ($n = 55$) or cells were examined using qRT-PCR or Western blotting. **k**–**m** Correlation among the levels of circ_0008035, miR-1184, and RAP2B in 50 cases of BC tissues. *$p < 0.05$.

Besides, circ_0008035 was mainly enriched in cytoplasm of 5,637 and T24 cells (Fig. 1d) and was resistant to RNase R digestion in contrast with its linear transcript EXT1 (Fig. 1e), which indicates that circ_0008035 is a stable circRNA that acts as a ceRNA for miRNA to function in cancers.

In addition, miR-1184 expression was decreased (Fig. 1f, g), while RAP2B mRNA and protein level were markedly enhanced in BC tissues and cells (Fig. 1h–j). Furthermore, the expression of miR-1184 in BC tissues was negatively associated with the expression of circ_0008035 and RAP2B, while the levels of circ_0008035 and RAP2B displayed a positive correlation in 55 cases of BC tissues (Fig. 1k–m).

Circ_0008035 Mediates Proliferation, Migration, Invasion, Angiogenesis, EMT, and Apoptosis in BC Cells

To investigate the biological effects of circ_0008035 on BC, rescue experiments were conducted in 5,637 and T24 cells by transfection of si-NC, si-circ_0008035#1, or si-circ_0008035#2. As exhibited in Figure 2a, the level of circ_0008035 was suppressed by half in cells with si-circ_0008035#1 or si-circ_0008035#2 transfection. Besides, circ_0008035 knockdown evidently inhibited the proliferation of 5,637 and T24 cells, as indicated by the reduced OD value (Fig. 2b), colony formation ability (Fig. 2c), and Edu-positive cells (Fig. 2d) in BC cells with si-circ_0008035#1 or si-circ_0008035#2 transfection.

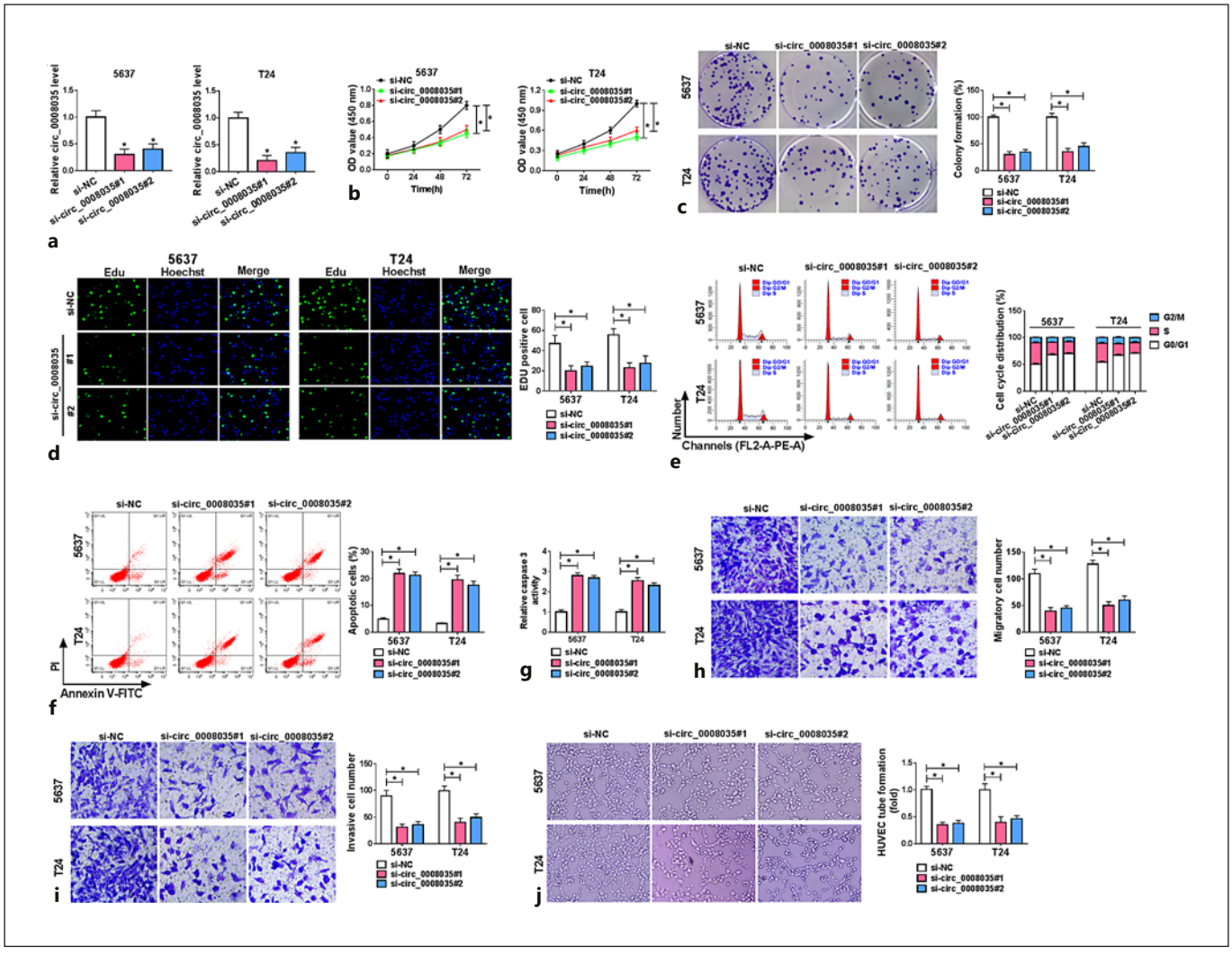

Fig. 2. Circ_0008035 knockdown mediates BC cell proliferation, cell cycle progression, apoptosis, migration, invasion, and angiogenesis. 5,637 and T24 cells were transfected with si-circ_0008035#1, si-circ_0008035#2, or si-NC, respectively. Circ_0008035 expression (**a**), cell proliferation (**b–d**), cell cycle distribution (**e**), apoptosis (**f**), caspase-3 activity (**g**), migration (**h**), invasion (**i**), and angiogenesis (**j**) were measured by qRT-PCR, CCK-8, colony formation, Edu staining, flow cytometry, caspase-3 assay kit, transwell, and tube formation assays, respectively. *$p < 0.05$. CCK-8, Cell Counting Kit-8.

Circ_0008035 knockdown also induced a G1 phase arrest in transfected BC cells (Fig. 2e, $p < 0.001$). Furthermore, the apoptosis rate and caspase-3 activity in 5,637 and T24 cells were elevated by circ_0008035 knockdown (Fig. 2f, g). Circ_0008035 knockdown greatly inhibited cell migration, invasion, and angiogenesis in 5,637 and T24 cells compared with si-NC group (Fig. 2h–j). What is more, we further investigated the effects of circ-0008035 on the malignant phenotype of BC cells via Western blot. As shown in online supplementary Figure 1, circ_0008035 knockdown caused the reduced expression of key proteins that enhanced progression through the cell cycle (CDK1, cyclin B1, and cyclin D1), which further identified that circ_0008035 knockdown induced cell cycle arrest in 5,637 and T24 cells. Besides, circ_0008035 knockdown suppressed the levels of anti-apoptotic protein Bcl-2, while it elevated the levels of pro-apoptotic protein (Bax) and apoptosis marker (cleaved caspase 3, 8, and 9). And cell motility was also suppressed by circ_0008035 knockdown, as indicated by the decreasing levels of motility-related proteins (MMP-7, MMP-2, and MMP-9). In addition, circ_0008035 knockdown in 5,637 and T24 cells

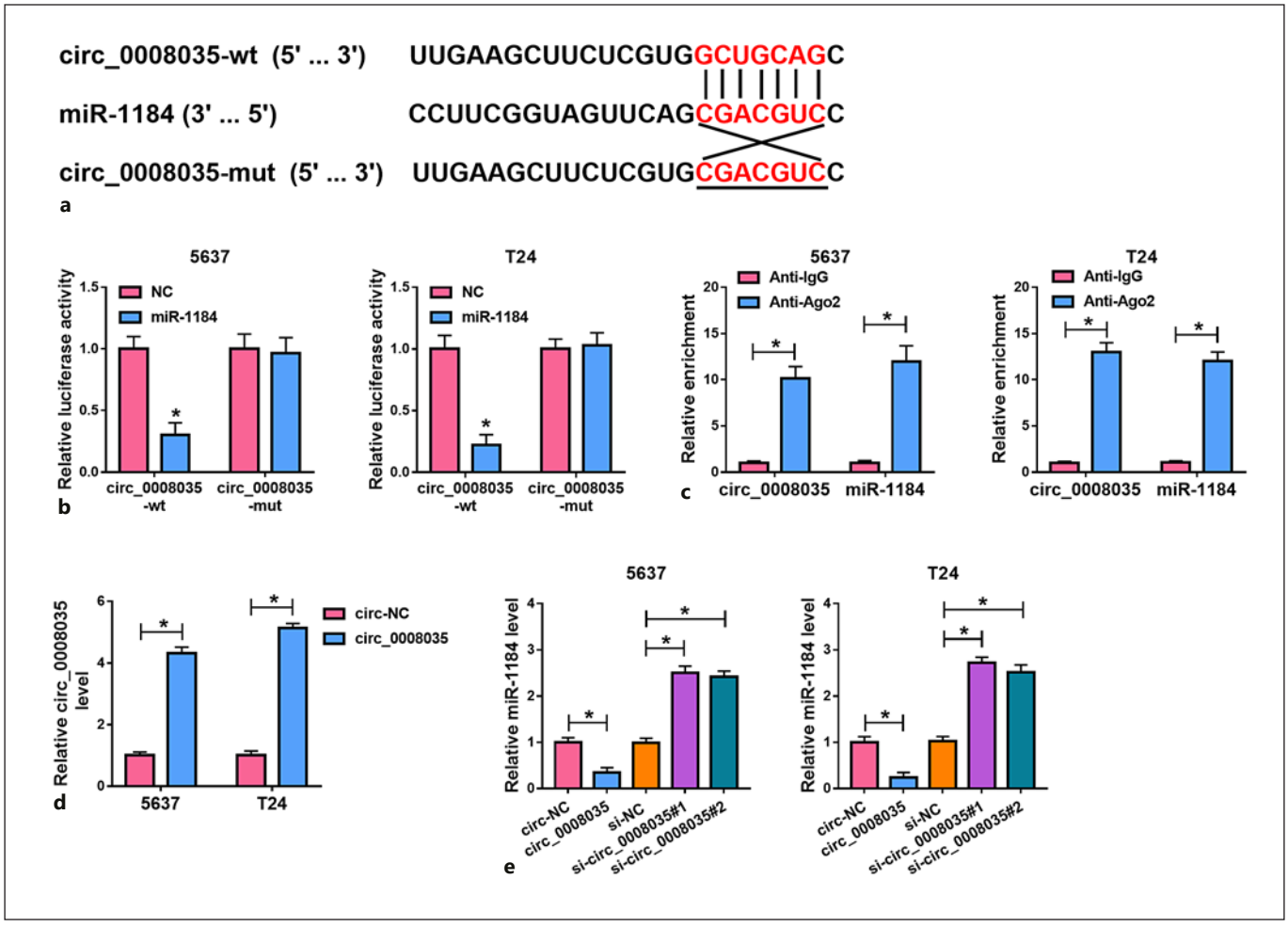

Fig. 3. Circ_0008035 acts as an endogenous sponge for miR-1184. **a** The binding sites between circ_0008035 and miR-1184. **b** Luciferase activity in 5,637 and T24 cells co-transfected with NC or miR-1184 mimic and circ_0008035-wt or circ_0008035-mut. **c** Circ_0008035 and miR-1184 enrichments in cells incubated with anti-Ago2 or anti-IgG were detected by RIP assay. **d** The level of circ_0008035 was examined by qRT-PCR in 5,637 and T24 cells transfected with circ-NC or circ_0008035 overexpression vector. **e** MiR-1184 level in 5,637 and T24 cells transfected with circ-NC, circ_0008035 overexpression vector, si-circ_0008035#1, si-circ_0008035#2, or si-NC was measured by qRT-PCR. *p < 0.05.

suppressed the EMT-like phenotype, which was evidenced by the improvement of E-cadherin and diminution of N-cadherin or vimentin expression at protein levels. Thus, circ_0008035 knockdown inhibited the progression of BC via regulating cell proliferation, cell cycle progression, apoptosis, migration, and invasion.

Moreover, overexpression of circ_0008035 promoted the proliferation of 5,637 and T24 cells, as the OD value, colony formation rate and Edu-positive cells were increased in cells with circ_0008035 overexpression vector transfection (online suppl. Fig. 2A–C). Moreover, overexpression of circ_0008035 increased the fraction of cells in S phase (online suppl. Fig. 2D), suppressed the apoptosis (online suppl. Fig. 2E), but promoted cell migration, invasion, and angiogenesis (online suppl. Fig. 2F–H) in 5,637 and T24 cells. Taken together, circ_0008035 functions as a tumor promoter in BC.

Circ_0008035 Acts as a Sponge for miR-1184 in BC Cells

To explore the potential mechanism addressed by circ_0008035 in BC cells, the target miRNA of miR-1184 was predicted by bioinformatics software Circinteractome. And miR-1184 was predicted to harbor the complementary binding sites of circ_0008035 (Fig. 3a). To verify this prediction, a dual-luciferase reporter assay was

performed, and the results showed that miR-1184 overexpression significantly reduced the luciferase activity of circ_0008035-wt group but not circ_0008035-mut group, in contrast with the miR-NC group (Fig. 3b). Besides, circ_0008035 and miR-1184 were enriched by Ago2 antibody, not the IgG antibody (Fig. 3c), which indicates the existence of circ_0008035 and miR-1184 in the RNA-induced silencing complex (RISC). Furthermore, 5,637 and T24 cells were transfected with circ-NC, circ_0008035 overexpression vector, si-NC, si-circ_0008035#1, or si-circ_0008035#2 to evaluate the effect of circ_0008035 on miR-1184 level. As shown in Figure 3d, circ_0008035 expression was 4-fold elevated in cells with circ_0008035 overexpression vector transfection. Furthermore, miR-1184 level was obviously decreased by circ_0008035 overexpression, but was increased by circ_0008035 knockdown (Fig. 3e). These research suggested that circ_0008035 negatively regulated miR-1184 by sponging miR-1184.

MiR-1184 Knockdown Reverses the Effects of circ_0008035 Knockdown on BC Progression

To investigate whether circ_0008035-mediated BC progression by regulating miR-1184, 5,637 and T24 cells were transfected with si-NC, si-circ_0008035#1, si-circ_0008035#1 + anti-NC, or anti-miR-1184. As shown in Figure 4a, b, miR-1184 level was suppressed by miR-1184 inhibitor and was upregulated by circ_0008035 knockdown. However, co-transfection of anti-miR-1184 and si-circ_0008035#1 reversed the promotion effect of circ_0008035 knockdown on miR-1184 level. Moreover, miR-1184 inhibitor partly attenuated circ_0008035 knockdown-mediated inhibition effects on 5,637 and T24 cell proliferation, as indicated by the elevated cell proliferation, colony formation ability, and Edu-positive ratio, while attenuating S phase cells ($p < 0.001$) (Fig. 4c–f). Additionally, miR-1184 downregulation alleviated the reducing apoptosis rate and caspase 3 activity in 5,637 and T24 cells that were mediated by circ_0008035 knockdown (Fig. 4g, h). Furthermore, miR-1184 knockdown mitigated the suppression effects of circ_0008035 knockdown on cell migration, invasion, and angiogenesis (Fig. 4i–k). These data revealed that circ_0008035 knockdown deregulates miR-1184 to repress BC progression.

MiR-1184 Targets RAP2B in BC

To explore the functional mechanism of miR-1184 in BC, the downstream targets of miR-1184 were analyzed by TargetScan. RAP2B 3′UTR sequence was predicted to contain the putative binding sites of miR-1184 (Fig. 5a). And it was further confirmed by dual-luciferase reporter assay. The luciferase activity of cells with miR-1184 mimic and RAP2B-wt co-transfection was significantly decreased, while the luciferase activity of RAP2B-mut group changed little in BC cells (Fig. 5b). Besides, the enrichment of miR-1184 and RAP2B in the Ago2-RIP group was especially enhanced compared with the anti-IgG group (Fig. 5c), indicating the presence of miR-1184 and RAP2B in the RISC. Additionally, miR-1184 level increased more than triple in cells with miR-1184 mimic transfection in contrast with the NC group (Fig. 5d). Moreover, miR-1184 mimic suppressed the protein level of RAP2B, while the protein level of RAP2B was upregulated by miR-1184 inhibitor (Fig. 5e). In addition, circ_0008035 knockdown decreased the protein level of RAP2B, while this tendency was restored by miR-1184 knockdown (Fig. 5f). Thus, RAP2B was targeted by miR-1184, and circ_0008035 regulates RAP2B expression by sponging miR-1184.

MiR-1184 Represses BC Progression by Regulating RAP2B

To explore the roles of miR-1184 and RAP2B in BC progression, 5,637 and T24 cells were transfected with NC, miR-1184 mimic, miR-1184 mimic + vector, or miR-1184 mimic + RAP2B overexpression vector, respectively. As exhibited in Figure 6a, the protein level of RAP2B was significantly elevated in cells with RAP2B overexpression vector transfection. Besides, RAP2B overexpression rescued the suppression effect of miR-1184 mimic on RAP2B protein levels in 5,637 and T24 cells (Fig. 6b). Moreover, miR-1184 overexpression significantly inhibited cell proliferation, reflected by decreased cell viability activity, colony formation ability, Edu-positive ratio, and arrest of S phase ($p < 0.05$), and RAP2B addition reversed this effect (Fig. 6c–f). Additionally, miR-1184 overexpression promoted cell apoptosis and caspase-3 activity, and this tendency was abrogated by RAP2B upregulation (Fig. 6g, h). Besides, miR-1184 mimic evidently decreased the abilities of cell migration and invasion, whereas RAP2B upregulation reversed this effect (Fig. 6i, j). In addition, RAP2B overexpression also mitigated the decreasing angiogenesis induced by miR-1184 mimic (Fig. 6k). Hence, miR-1184 repressed BC progression by regulating RAP2B.

Circ_0008035 Silencing Curbs BC Tumor Growth in vivo

To investigate the functional effect of circ_0008035 on BC development in vivo, the xenograft model was established by injecting 5,637 and T24 cells stably transfected

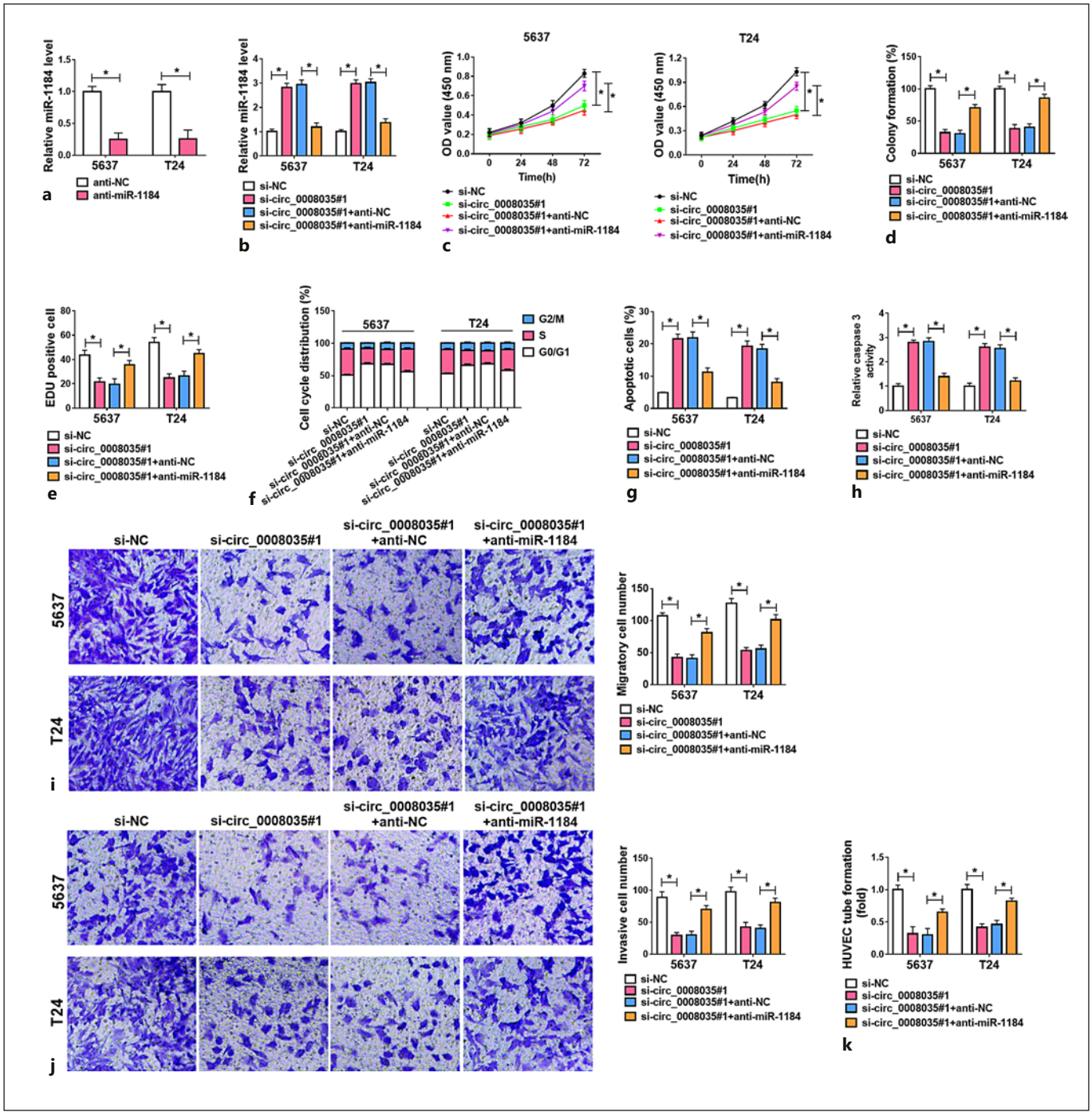

Fig. 4. Circ_0008035 regulates the progression of BC by sponging miR-1184. **a** MiR-1184 expression was detected by qRT-PCR in 5,637 and T24 cells transfected with anti-NC or anti-miR-1184. **b–k** 5,637 and T24 cells were transfected with si-NC, si-circ_0008035#1,si-circ_0008035#1+anti-NC,orsi-circ_0008035#1 + anti-miR-1184, respectively. The expression of miR-1184 (**b**), cell proliferation (**c–e**), cell cycle progression (**f**), apoptosis (**g**), caspase-3 activity (**h**), migration (**i**), invasion (**j**), and angiogenesis (**k**) were measured by qRT-PCR, CCK-8, colony formation, Edu staining, flow cytometry, caspase-3 assay kit, transwell, and tube formation assays, respectively. *$p < 0.05$. CCK-8, Cell Counting Kit-8.

with sh-circ_0008035 or sh-NC into nude mice (n = 5 per group). After a 5-week observation, tumor volume and weight obviously decreased in sh-circ_0008035 group compared with sh-NC group (Fig. 7a, b). Additionally, circ_0008035 and RAP2B protein levels were markedly decreased, while miR-1184 level was evidently upregulated in sh-circ_0008035 group (Fig. 7c–e). Moreover, ki-67 IHC staining of xenograft tumors with circ_0008035 silencing indicated a reduced proliferation in contrast with the control group (Fig. 7f), as indicated by the percentage of ki-67 positive cells in tumor cells. Taken together, circ_0008035 silencing constrained the growth of BC tumors in vivo.

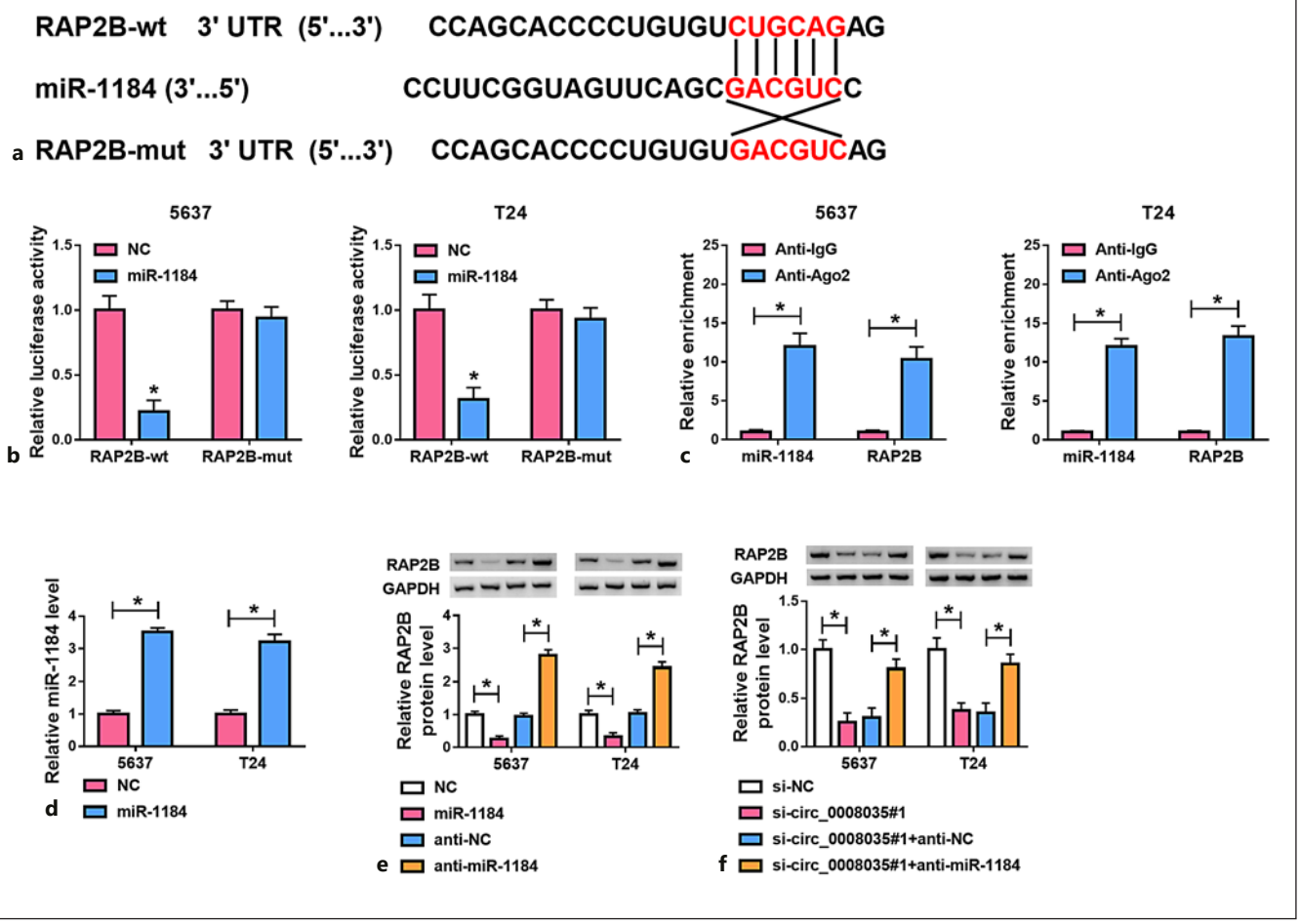

Fig. 5. RAP2B is targeted by miR-1184. **a** The putative binding sites of miR-1184 in RAP2B 3′UTR. **b** Luciferase activity in 5,637 and T24 cells co-transfected with NC or miR-1184 mimic and RAP2B-wt or RAP2B-mut. **c** The enrichment of miR-1184 and RAP2B in 5,637 and T24 cells incubated with Ago2 or IgG antibodies were detected by Ago2-RIP assay. **d** MiR-1184 expression was detected via qRT-PCR in 5,637 and T24 cells transfected with NC or miR-1184 mimic. **e** RAP2B protein level was detected in cells with transfection of NC, miR-1184 mimic, anti-NC or anti-miR-1184. **f** RAP2B protein level was examined in 5,637 and T24 cells with transfection of si-NC, si-circ_0008035#1, si-circ_0008035#1 + anti-NC, or si-circ_0008035#1 + anti-miR-1184. *$p < 0.05$.

Fig. 6. RAP2B mediates the functions of miR-1184 in BC progression. **a** The protein level of RAP2B was detected using Western blotting in cells transfected with vector or RAP2B overexpression vector. **b–k** 5,637 and T24 cells were transfected with NC, miR-1184 mimic, miR-1184 mimic + vector, or miR-1184 mimic + RAP2B overexpression vector, respectively. Western blotting, CCK-8, colony formation, Edu staining, flow cytometry, caspase-3 assay kit, transwell, and tube formation assays were conducted to evaluate the protein level of RAP2B (**b**), cell proliferation (**c–e**), cell cycle progression (**f**), apoptosis (**g**), caspase-3 activity (**h**), migration (**i**), invasion (**j**), and angiogenesis (**k**) in transfected cells. *$p < 0.05$. CCK-8, Cell Counting Kit-8.

(For figure see next page.)

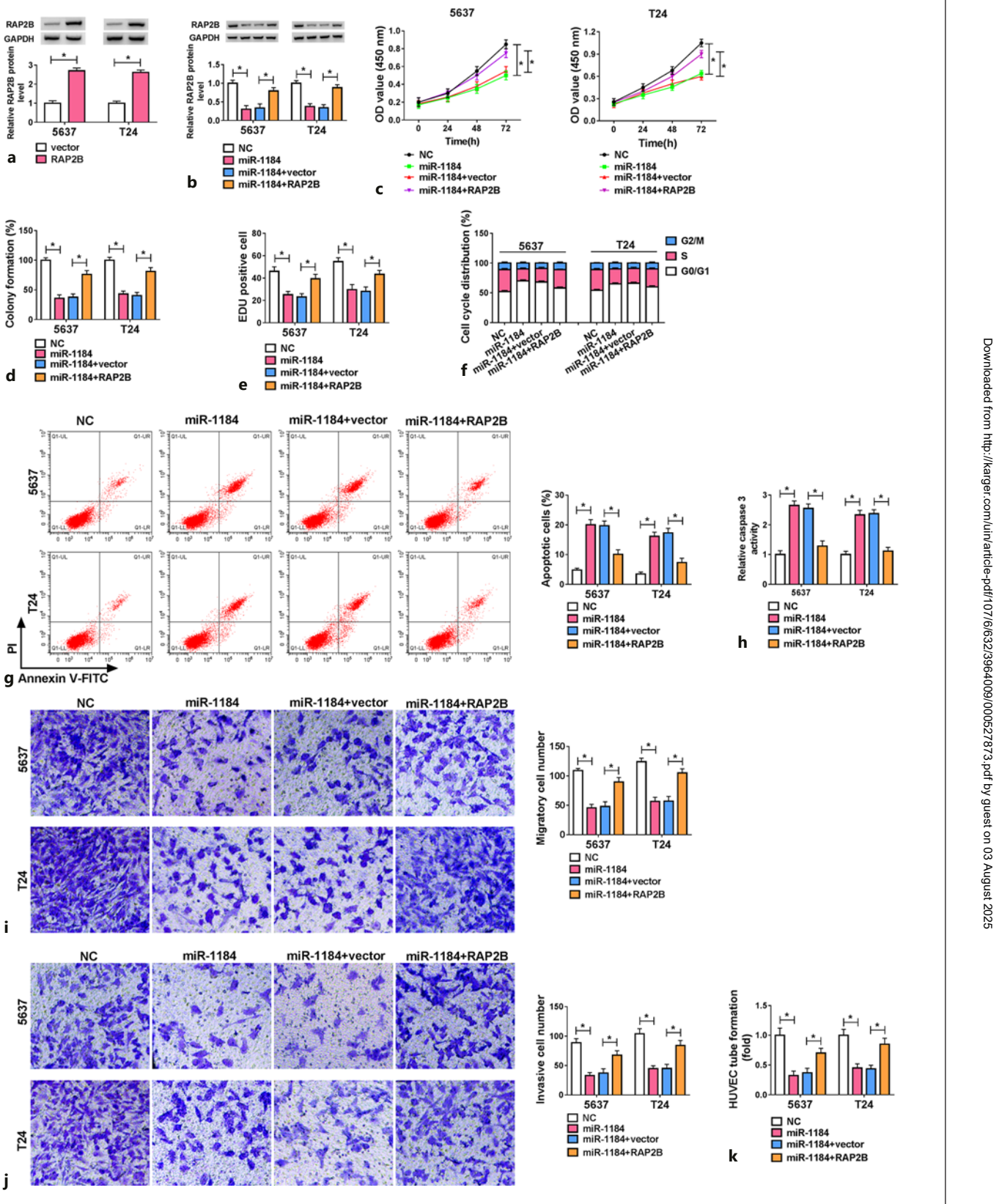

6

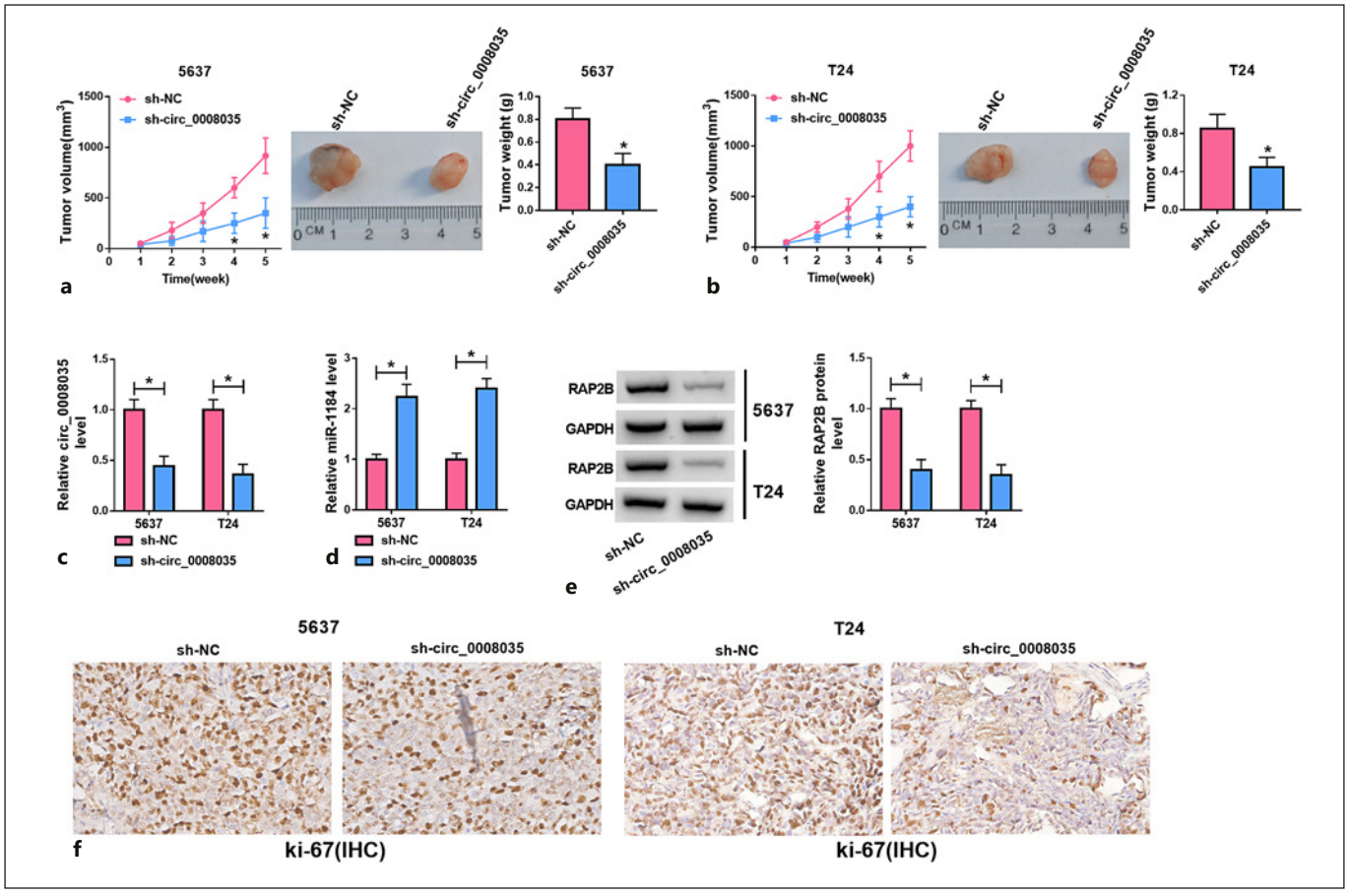

Fig. 7. Circ_0008035 silencing inhibits BC tumor growth in vivo. 5,637 and T24 cells stable transfected with sh-circ_0008035 or sh-NC were injected into the nude mice to establish a xenograft model (5 mice for each group). Five weeks upon injection, (**a**, **b**) tumor volume and weight, (**c–e**) as well as circ_0008035, miR-1184 and RAP2B levels in xenograft tumor tissues were measured. **f** IHC staining for ki-67 was employed to evaluate the proliferation of tumor cells in xenograft tumor tissues. *$p < 0.05$.

Discussion

CircRNAs are involved in various tumor biological processes, which provides a novel therapeutic strategy for BC treatment [17]. In our study, circ_0008035 expression was increased in BC and was closely related to the metastasis of BC tumor. Loss-of-function experiments uncovered that circ_0008035 knockdown constrained cell proliferation, migration, invasion, EMT process, and angiogenesis but promoted apoptosis in BC cells. Moreover, circ_0008035 functioned as a sponge for miR-1184 to upregulate RAP2B expression, thereby promoting the progression of BC.

Huang et al. [18] reported that circ_0008035 could promote cell proliferation and invasion via regulating miR-375 and Y-box binding protein 1 (YBX1) in gastric cancer. Li et al. [19] suggested that circ_0008035 contributed to cell proliferation but inhibited apoptosis and ferroptosis by modulating miR-599 and eukaryotic initiation factor 4A1 (EIF4A1) in gastric cancer. Moreover, Gong et al. [20] suggested that circ_0008035 promoted cell growth and migration in osteosarcoma via regulating miR-375 and Notch signaling. A previous report suggested circ_0008035 expression was increased in BC patients [10]. The growth and metastasis are the main malignancies of BC [21, 22]. Tumor-related blood vessels differ from normal vessels, and the angiogenesis is responsible for tumor growth and metastasis in BC [23, 24]. Hence, we investigated the effects of circ_0008035 on cell growth, metastasis, and angiogenesis in BC. Loss-of-function experiments suggested circ_0008035 downregulation restrained cell proliferation, migration, invasion, and angiogenesis but promoted apoptosis in BC cells, whereas circ_0008035 overexpression

promoted the progression of BC cells. Additionally, circ_0008035 silencing also curbed the growth of BC in vivo. EMT is a developmental program, which has been involved in carcinogenesis and confers metastatic properties upon cancer cells by enhancing mobility, invasion, and resistance to apoptotic stimuli [25]. EMT contributes to cancer migration, invasion, and metastatic outgrowth, and this work also showed that circ_0008035 knockdown inhibited EMT process to impede BC metastasis. In all, the use of circ_0008035 siRNA or shRNA might be a promising therapeutic strategy for BC. siRNA can selectively silence a pathological pathway via the targeting and degradation of a specific mRNA. However, there are two major problems that limit the application of siRNA: the delivery systems and unwanted side effects induced by siRNA. Currently, emerging findings have proposed that nanocarriers based delivery of siRNA has the advantage to overcome physiological barriers and protect siRNA integrity [26, 27]. Besides that, siRNA redundancy chemical modification such as 2′-O-methyl or 2′-fluoro modification have been identified that may mitigate the side effects of the interferon response and off-target effects [28, 29], further indicating the potential clinical application of siRNA in disease treatment.

Several research has disclosed the pivotal role of circ_0008035-mediated ceRNA networks in cancers [18, 19]. In current research, circ_0008035 is mainly located in cytoplasm, which may function as a microRNA sponge in BC. The results of dual-luciferase reporter assay showed that miR-1184 overexpression significantly reduced the luciferase activity of wild-type circ_0008035 vector. Besides, RISC mediates post-transcriptional control of gene expression and contains Ago2 protein as a central effector of cleavage or inhibition of mRNA translation. We confirmed circ_0008035 and miR-1184 were enriched by Ago2 antibody but not the IgG antibody, suggesting the existence of circ_0008035 and miR-1184 in the RISC. Thus, we verified that miR-1184 was a target of circ_0008035 and could be absorbed by circ_0008035. Chen et al. [30] suggested miR-1184 inhibited cell proliferation and promoted apoptosis by regulating casein kinase 2 alpha 1 (CSNK2A1) in colon cancer. Furthermore, miR-1184 suppressed cell proliferation, migration, and invasion via targeting ajuba LIM protein (AJUBA) in colorectal cancer [31]. Moreover, miR-1184 could repress proliferation, migration, and invasion through modulating insulin-like growth factor binding protein 2 (IGFBP2) or integrin α3 (ITGA3) in BC [13, 32]. In accordance with previous research, miR-1184 acted as a tumor suppressor in BC by regulating cell proliferation, migration, invasion, and angiogenesis. Circ_0008035 could regulate BC development via sponging miR-1184.

Then we further explored the downstream pathway of miR-1184, and we confirmed that miR-1184 could target RAP2B in BC. RAP2B has been reported to act as an oncogene, which increases cell proliferation, migration, and invasion in multiple tumors, like prostate cancer, hepatocellular carcinoma, and cervical cancer [33–35]. Furthermore, RAP2B promotes angiogenesis by activating the phosphoinositide 3-kinase (PI3K)/protein kinase B (AKT)/vascular endothelial growth factor (VEGF) pathway in renal cell carcinoma [36]. More importantly, Zhang et al. [15] reported that RAP2B was highly expressed in BC, and its knockdown inhibited BC cell proliferation and invasion, suggesting the carcinogenic role of RAP2B in BC. Here we revealed that miR-1184 suppressed BC progression through targeting RAP2B. Furthermore, circ_0008035 could serve as a ceRNA for miR-1184 to upregulate RAP2B expression. In conclusion, circ_0008035 was highly expressed in BC, and circ_0008035 promotes BC progression via serving as a ceRNA for miR-1184 to modulate RAP2B expression, which indicates a novel insight into the therapeutic target for BC.

Statement of Ethics

Written informed consents were obtained from all participants and this study was permitted by the Ethics Committee of The Second Hospital of The Affiliated Huaian No. 1 People's Hospital of Nanjing Medical University (IRB No. 2019HA557).

Conflict of Interest Statement

The authors declare that they have no conflict of interest.

Funding Sources

This manuscript did not receive any funding.

Author Contributions

Yang Fu designed and performed the research; Kun Liu, Xi Jiang, Lun Zhao, Tianwei Wang analyzed the data; Yang Fu wrote the manuscript. All authors read and approved the final manuscript.

Data Availability Statement

All data generated or analyzed during this study are included in this article and its online supplementary material. Further inquiries can be directed to the corresponding author.

References

1 Kamat AM, Hahn NM, Efstathiou JA, Lerner SP, Malmstrom PU, Choi W, et al. Bladder cancer. Lancet. 2016;388(10061):2796–810.
2 Heath EI, Rosenberg JE. The biology and rationale of targeting nectin-4 in urothelial carcinoma. Nat Rev Urol. 2021;18(2):93–103.
3 Antoni S, Ferlay J, Soerjomataram I, Znaor A, Jemal A, Bray F. Bladder cancer incidence and mortality: a global overview and recent trends. Eur Urol. 2017;71(1):96–108.
4 Su H, Jiang H, Tao T, Kang X, Zhang X, Kang D, et al. Hope and challenge: Precision medicine in bladder cancer. Cancer Med. 2019;8(4):1806–16.
5 Simion V, Zhou H, Pierce JB, Yang D, Haemmig S, Tesmenitsky Y, et al. LncRNA VINAS regulates atherosclerosis by modulating NF-κB and MAPK signaling. JCI Insight. 2020;5(21):e140627.
6 Li C, Fu X, He H, Chen C, Wang Y, He L. The biogenesis, functions, and roles of circRNAs in bladder cancer. Cancer Manag Res. 2020;12:3673–89.
7 Jiang WD, Yuan PC. Molecular network-based identification of competing endogenous RNAs in bladder cancer. PLoS One. 2019;14(8):e0220118.
8 Jin M, Lu S, Wu Y, Yang C, Shi C, Wang Y, et al. Hsa_circ_0001944 promotes the growth and metastasis in bladder cancer cells by acting as a competitive endogenous RNA for miR-548. J Exp Clin Cancer Res. 2020;39(1):186.
9 Liu Z, Yang Y, Yang Z, Xia S, Lin D, Xiao B, et al. Novel circRNA_0071196/miRNA19b3p/CIT axis is associated with proliferation and migration of bladder cancer. Int J Oncol. 2020;57(3):767–79.
10 Zhong Z, Lv M, Chen J. Screening differential circular RNA expression profiles reveals the regulatory role of circTCF25-miR-103a-3p/miR-107-CDK6 pathway in bladder carcinoma. Sci Rep. 2016;6(1):30919.
11 Blanca A, Cheng L, Montironi R, Moch H, Massari F, Fiorentino M, et al. Mirna expression in bladder cancer and their potential role in clinical practice. Curr Drug Metab. 2017;18(8):712–22.
12 Parizi PK, Yarahmadi F, Tabar HM, Hosseini Z, Sarli A, Kia N, et al. MicroRNAs and target molecules in bladder cancer. Med Oncol. 2020;37(12):118.
13 Yang D, Qian H, Fang Z, Xu A, Zhao S, Liu B, et al. Silencing circular RNA VANGL1 inhibits progression of bladder cancer by regulating miR-1184/IGFBP2 axis. Cancer Med. 2020;9(2):700–10.
14 Qu D, Huang H, Di J, Gao K, Lu Z, Zheng J. Structure, functional regulation and signaling properties of Rap2B. Oncol Lett. 2016;11(4):2339–46.
15 Zhang M, Zhuang Q, Cui L. MiR-194 inhibits cell proliferation and invasion via repression of RAP2B in bladder cancer. Biomed Pharmacother. 2016;80:268–75.
16 Livak KJ, Schmittgen TD. Analysis of relative gene expression data using real-time quantitative PCR and the 2−ΔΔCT method. Methods. 2001;25(4):402–8.
17 Cai Z, Li H. Circular RNAs and Bladder Cancer. Onco Targets Ther. 2020;13:9573–86.
18 Huang S, Zhang X, Guan B, Sun P, Hong CT, Peng J, et al. A novel circular RNA hsa_circ_0008035 contributes to gastric cancer tumorigenesis through targeting the miR-375/YBX1 axis. Am J Transl Res. 2019;11(4):2455–62.
19 Li C, Tian Y, Liang Y, Li Q. Circ_0008035 contributes to cell proliferation and inhibits apoptosis and ferroptosis in gastric cancer via miR-599/EIF4A1 axis. Cancer Cel Int. 2020;20(1):84.
20 Gong G, Han Z, Wang W, Xu Q, Zhang J. Silencing hsa_circRNA_0008035 exerted repressive function on osteosarcoma cell growth and migration by upregulating microRNA-375. Cell Cycle. 2020;19(17):2139–47.
21 Chen Z, Yang L, Chen L, Li J, Zhang F, Xing Y, et al. miR-190b promotes tumor growth and metastasis via suppressing NLRC3 in bladder carcinoma. FASEB J. 2020;34(3):4072–84.
22 Wang X, Zhang H, Yang H, Bai M, Ning T, Deng T, et al. Exosome-delivered circRNA promotes glycolysis to induce chemoresistance through the miR-122-PKM2 axis in colorectal cancer. Mol Oncol. 2020;14(3):539–55.
23 Fus LP, Gornicka B. Role of angiogenesis in urothelial bladder carcinoma. Cent Eur J Urol. 2016;69(3):258–63.
24 Roudnicky F, Poyet C, Buser L, Saba K, Wild P, Otto VI, et al. Characterization of tumor blood vasculature expression of human invasive bladder cancer by laser capture microdissection and transcriptional profiling. Am J Pathol. 2020;190(9):1960–70.
25 Mittal V. Epithelial mesenchymal transition in tumor metastasis. Annu Rev Pathol Mech Dis. 2018;13(1):395–412.
26 Amadio M, Pascale A, Cupri S, Pignatello R, Osera C, D Agata V, et al. Nanosystems based on siRNA silencing HuR expression counteract diabetic retinopathy in rat. Pharmacol Res. 2016;111:713–20.
27 Bardoliwala D, Patel V, Javia A, Ghosh S, Patel A, Misra A. Nanocarriers in effective pulmonary delivery of siRNA: current approaches and challenges. Ther Deliv. 2019;10(5):311–32.
28 Scaggiante B, Dapas B, Farra R, Grassi M, Pozzato G, Giansante C, et al. Improving siRNA bio-distribution and minimizing side effects. Curr Drug Metab. 2011;12(1):11–23.
29 Jackson AL, Linsley PS. Recognizing and avoiding siRNA off-target effects for target identification and therapeutic application. Nat Rev Drug Discov. 2010;9(1):57–67.
30 Yang J, Zhang Z, Chen S, Dou W, Xie R, Gao J. miR-654-3p predicts the prognosis of hepatocellular carcinoma and inhibits the proliferation, migration, and invasion of cancer cells. Cancer Biomark. 2020;28(1):73–9.
31 Zhang H, Shen Z, Zhou Y, Zhang Z, Wang Q, Zhang M, et al. Downregulation of miR-654-3p in colorectal cancer indicates poor prognosis and promotes cell proliferation and invasion by targeting SRC. Front Genet. 2020;11:577948.
32 Jiang P, Zhu Y, Xu Z, Chen X, Xie L. Interference with circBC048201 inhibits the proliferation, migration, and invasion of bladder cancer cells through the miR-1184/ITGA3 axis. Mol Cel Biochem. 2020;474(1–2):83–94.
33 Di J, Cao H, Tang J, Lu Z, Gao K, Zhu Z, et al. Rap2B promotes cell proliferation, migration and invasion in prostate cancer. Med Oncol. 2016;33(6):58.
34 Zhang L, Duan HB, Yang YS. Knockdown of Rap2B inhibits the proliferation and invasion in hepatocellular carcinoma cells. Oncol Res. 2017;25(1):19–27.
35 Li Y, Li S, Huang L. Knockdown of Rap2B, a Ras superfamily protein, inhibits proliferation, migration, and invasion in cervical cancer cells via regulating the ERK1/2 signaling pathway. Oncol Res. 2018;26(1):123–30.
36 Di J, Gao K, Qu D, Wu Y, Yang J, Zheng J. Rap2B promotes angiogenesis via PI3K/AKT/VEGF signaling pathway in human renal cell carcinoma. Tumour Biol. 2017;39(7):101042831770165.